Journal of Alloys and Compounds, 194 (1993) 1–7
JALCOM 541

Alloying behaviour among U, Np, Pu and Am predicted with the Brewer valence bond model

Toru Ogawa
Japan Atomic Energy Research Institute, Tokai-mura, Naka-gun, Ibaraki-ken 319-11 (Japan)

(Received July 8, 1992)

Abstract

The Brewer valence bond model allows estimation of the interaction between metal atoms. The model was applied to predict the alloying behaviour among actinides. It was found that the model correctly predicts the high temperature constitutions of binary alloys between actinides, which involve the liquid, b.c.c. and f.c.c. phases. Besides, recent experimental observations on the U–Am and Np–Am systems were reasonably explained. The only exception was the U–Pu system, where a significant negative interaction term has to be assumed in order to explain the experimental liquidus and solidus. Predictions for the ternary systems U–Pu–Am and Np–Pu–Am were also made.

1. Introduction

Recent interest in the nuclear transmutation of transuranium elements has identified the need for a database of the constitution of their alloys [1]. Although study of the experimental phase diagrams of these systems has been renewed, we will not be able to obtain a comprehensive compilation in the near future owing to the radiological toxicity of the transuranium elements. A proper combination of experimental and computational approaches is particularly desirable for these alloy systems.

In order to calculate an alloy phase diagram, the excess free energy of mixing (ΔG^{E}) for each phase has to be known. Several models for estimating ΔG^{E} have been proposed in the past [2–4]. Among them, the valence bond model of Brewer [4–8] is characterized by (1) its correlation of thermodynamic properties with electronic structures and (2) its relative independence from empirical fitting parameters. These characteristics of the Brewer model are attractive in the study of the alloying behaviour of transuranium elements. In this study the Brewer model was applied to the binary systems among U, Np, Pu and Am. As described in the following, the predictions of the model compare favourably with experimental phase diagrams in the literature as well as recent observations on the U–Am and Np–Am systems.

The ternary systems U–Pu–Am and Np–Pu–Am are of more technological importance, because the concepts of actinide burner reactors assume the use of either a U–Pu-based alloy fuel [9] or a combination of Np- and Am-based alloy fuels [10]. Both the U–Am and Np–Am binaries are characterized by poor miscibility. The effects of Pu addition on their miscibility were investigated.

The Brewer model is apparently incongruous with the current physical understanding of the cohesion of transition and actinide metals, which stresses the importance of band structure. The band structure terms are neglected in the Brewer model, though this defect is partly offset by the use of empirical cohesive energies and molar volumes. Since the alternative physical models do not seem to be accurate enough to provide the free-energy change on alloying, the predictive capability of the Brewer model remains attractive and warrants further investigation.

2. Analysis

The model described below follows the treatment of the alloys of Mo with Sc, Y and lanthanides by Brewer and Lamoreaux [6]. It is basically a regular solution model with interaction parameters derived from the Brewer valence bond theory. The interaction parameters are related to the "internal pressures" of the elements, $\Delta E^{*}/V$, where ΔE^{*} is the atomization energy to the gaseous valance state of the element and V is the molar volume. The gaseous valence state is defined as the state of gas atoms with the same electronic configuration as in the given condensed phase.

0925-8388/93/$6.00

Brewer discusses the relation of the crystal structure of metals and alloys with the electronic configuration, particularly with the number of unpaired s- and p-electrons [4]. Then the valence states of metal elements with typical structures were assigned [4, 7]. ΔE^* is taken to be the sum of the atomization energy to the gaseous ground state and the promotion energy of gas atoms from the ground state to an excited state corresponding to the given valence state. The promotion energies are estimated from spectroscopic data and are given in his compilations [7, 8]. For the liquid metals the compilation is given by Lamoreaux [11].

In the present study, extension of the regular solution model to the ternary alloys was made with the use of the Redlich–Kister–Muggianu (RKM) formulation [12], where the excess Gibbs energy of mixing is given by

$$\Delta G^{\mathrm{E}} = \sum_{i=1}^{n-1} \sum_{j=i+1}^{n} \sum_{p=0}^{m_{ij}} A_{ij}^{p} X_i X_j (X_i - X_j)^p + \sum_{i=1}^{n-2} \sum_{j=i+1}^{n-1} \sum_{k=j+1}^{n} C_{ijk} X_i X_j X_k \quad (1)$$

Here n is the number of components, m_{ij} is the degree of polynomial for A_{ij}^{p}, A_{ij}^{p} is the pth polynomial coefficient for a binary pair i–j, X_i, X_j and X_k are the mole fractions of components i, j and k respectively and C_{ijk} are coefficients of the ternary correction term. The RKM interaction parameter for a binary pair i–j, A_{ij}, was assumed to be of the first degree, *i.e.* $m_{ij}=1$ and only A_{ij}^{0} and A_{ij}^{1} were taken into account. The ternary correction term was neglected, *i.e.* $C_{ijk}=0$.

According to the Brewer model [6], the coefficients A_{ij}^{0} and A_{ij}^{1} are related to the internal pressures of the elements:

$$\alpha = \frac{V_i}{2}\left[\left(\frac{\Delta E_i^*}{V_i}\right)^{1/2} - \left(\frac{\Delta E_j^*}{V_j}\right)^{1/2}\right]^2 \quad (2)$$

$$\beta = \frac{2(V_j - V_i)}{V_i - 2V_j} \quad (3)$$

$$A_{ij}^{0} = \alpha + A_{ij}^{1} \quad (4)$$

$$A_{ij}^{1} = \frac{-\beta\alpha}{4(1+\beta)} \quad (5)$$

The values of ΔE^* and V adopted in this study are given in Table 1. Only the liquid, b.c.c. and f.c.c. phases were considered. Since the values for the f.c.c. phases of U and Np are not given by Brewer, they were estimated here by assuming the $d^{0.5}s^1p^{1.5}$ configuration for the f.c.c. structure as for f.c.c.-Pu. In the estimation we referred to the compilation of possible bonding configurations of the actinides [8].

Recently, Haire and Gibson [13] have confirmed the β–γ transition of Am by differential thermal analysis (DTA). In the following the γ phase is assumed to be a b.c.c. phase, which may be assigned the f^6d^2s configuration. The total number of s- and p-electrons should be 1–1.5 according to the Brewer valence bond model. However, there are large uncertainties (± 25 kJ mol^{-1}) in the promotion energies of Am [8]. In this study the value for the f^6dsp configuration given by Lamoreaux [11] was assumed invariably for the liquid, b.c.c. and f.c.c. phases of Am.

The molar volumes V in Table 1 are the room temperature values taken from ref. 14. The volume changes at fusion are as given by Lamoreaux [11].

The resulting RKM interaction parameters are given in Table 2. The excess entropy term associated with the temperature coefficients of the energies of vaporization and the molar volume was neglected. The free energies of transformation are given in Table 3. The equilibrium calculations were made with the Gibbs free-energy minimizer ChemSage [15].

TABLE 1. Atomization energies to the valence state (ΔE^*) and molecular volumes (V) of actinide metals

Element	Form	Assumed valence				ΔE^* (kJ mol^{-1})	V (cm^3 mol^{-1})
		f	d	s	p		
U	Liquid	1	4	1	0	767.35	13.78
	B.c.c.	1	4	1	0	776.55	12.65
	F.c.c.	3	0.5	1	1.5	802.91	(12.65)
Np	Liquid	3	3	1	0	708.77	13.1
	B.c.c.	3	3	1	0	714.63	12.16
	F.c.c.	4	0.5	1	1.5	694.47	(12.16)
Pu	Liquid	5	1.5	1	0.5	543.50	14.53
	B.c.c.	5	1.5	1	0.5	546.85	13.75
	F.c.c.	5	0.5	1	1.5	609.19	15.02
Am	Liquid	6	1	1	1	609.19	18.5
	B.c.c.					623.42	(17.64)
	F.c.c.					629.27	17.64

3. Results and discussion

In the following the calculated phase diagrams are compared with the experimental ones. Except for the U–Pu system the calculations agreed or compared favourably with the experimental observations. The binaries other than U–Pu are discussed first and then the latter system is considered. Finally, predictions for the ternary systems U–Pu–Am and Np–Pu–Am are made.

3.1. U–Np and Np–Pu

Complete solubilities have been found for the liquid and b.c.c. phases of the U–Np [16] and Np–Pu [17]

TABLE 2. RKM interaction parameters for alloys of U, Np, Pu and Am (for U–Pu see text)

Phase	Pair	A^0 (J mol^{-1})	A^1 (J mol^{-1})	Remarks
Liquid	U–Np	76.5	−1.94	
	U–Pu	0	0	Assumed
	U–Am	23982	3507	
	Pu–Np	10614	−549	
	Pu–Am	1177	141.5	
	Np–Am	20661	3531	
B.c.c.	U–Np	177	−3.5	
	U–Pu	3600	−1300	Fitted
	U–Am	27055	4457	
	Pu–Np	11975	−735	
	Pu–Am	1026	127.1	
	Np–Am	22072	4059	
F.c.c.	U–Np	960	−19.0	
	U–Pu	(3600)	(−1300)	Assumed
	U–Am	30114	4961	
	Pu–Np	9866	−1038	
	Pu–Am	1280	102.7	
	Np–Am	19091	3511	

TABLE 3. Free energies of transformation (ΔG_t)

Element	Transformation	ΔG_t (J mol^{-1})
U	B.c.c. → liquid	$9142-6.485T$
Np	B.c.c. → liquid	$5188-5.69T$
Pu	B.c.c. → liquid	$2824.2-3.093T$
	F.c.c. → b.c.c.	$1926-2.554T$
Am	B.c.c. → liquid	$14393-9.933T$
	F.c.c. → b.c.c.	$5862-4.343T$

systems. The experimental solidus–liquidus curves (dashed curves in Figs. 1 and 2) have been drawn principally on the basis of the thermal analyses. The study by Mardon *et al.* [17] on the Np–Pu system confirmed the b.c.c. structure of γ-Np for the first time. The complete solubility in the b.c.c. phase of the U–Np system has been inferred from the thermal analysis [16] and the later structure assignment of γ-Np, since the authors could not make satisfactory X-ray diffraction measurements on the U–Np alloys.

The liquid–b.c.c. equilibria were predicted accurately with the model calculation as seen in Figs. 1 and 2 (solid curves). The liquid and b.c.c. solutions between U and Np are almost ideal: the interaction parameters are of the order of 0.1 kJ mol^{-1}. On the other hand, a shallow depression in the solidus–liquidus curves in the middle of the Np–Pu system is noted. This depression is explained by the interaction parameter of the b.c.c. phase being more positive by about 1 kJ mol^{-1} than that of the liquid phase.

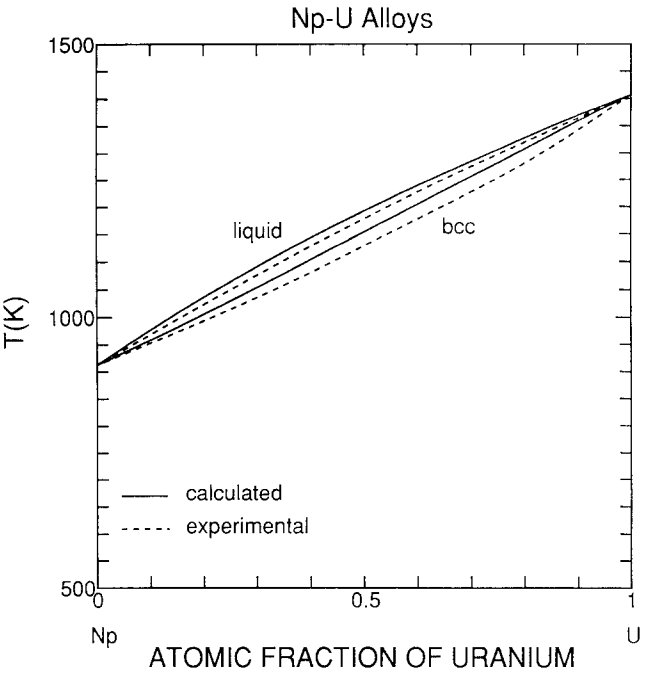

Fig. 1. Liquid–b.c.c. equilibrium in the U–Np system.

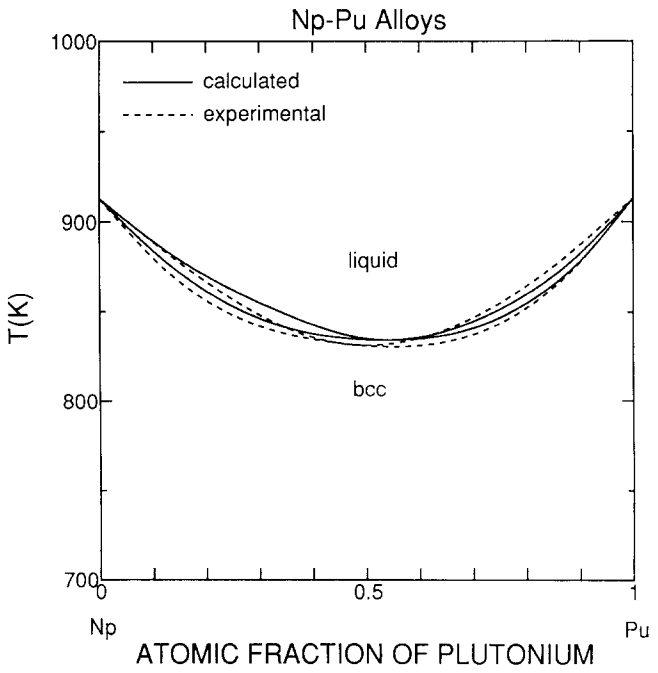

Fig. 2. Liquid–b.c.c. equilibrium in the Np–Pu system.

3.2. *U–Am and Np–Am*

There are no phase diagrams for these systems in the literature. Inoue *et al.* [18] reported that an attempt to fuse a nearly equimolar mixture of U and Am failed, giving an inhomogeneous mass consisting of apparently immiscible phases. Figure 3 gives the model prediction for this system, which is characterized by a liquid miscibility gap with a monotectic horizontal at about

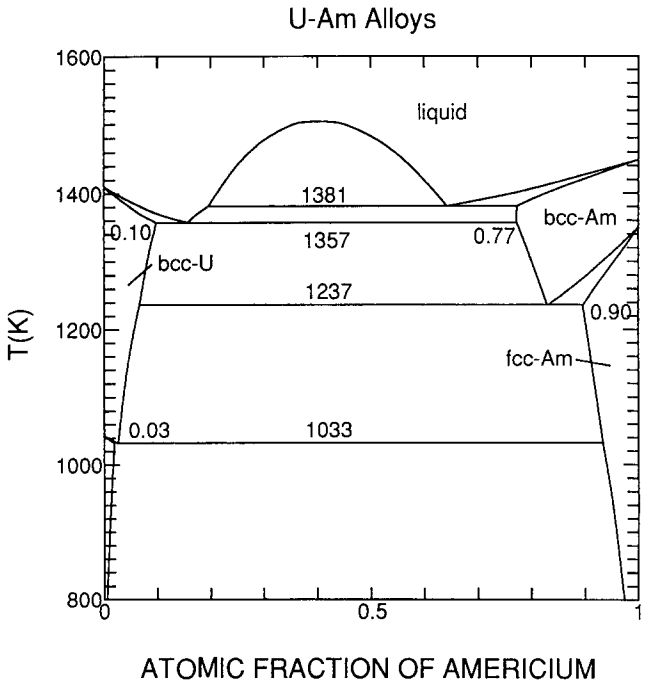

Fig. 3. Predicted phase diagram of the U–Am system.

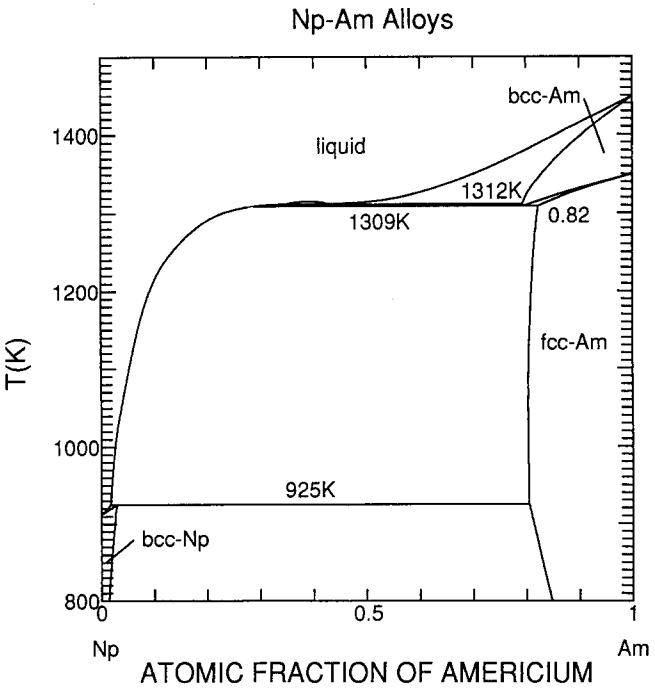

Fig. 4. Predicted phase diagram of the Np–Am system.

1380 K. A greater solubility of U in Am than vice versa is predicted.

Haire and Gibson [13] have made a series of DTA measurements on pure Np and Am and on a 54at.%Np–46at.%Am mixture. After repeated heating of the mixture to 1473 K, they observed DTA peaks corresponding to the three allotropic transformations of Np and two additional peaks which are considered to be related to the β(f.c.c.)–γ transition and the fusion of the Am-based phases. For the latter two peaks the β–γ onset temperature was depressed by about 60 K and the liquidus onset by about 150 K from those of pure Am, with the result that the DTA peaks of the two transitions almost merged into a narrow doublet at 1253–1293 K.

Figure 4 shows the model prediction for the Np–Am system, which is monotectic with a barely noticeable liquid miscibility gap. The model predicts a greater solubility of Np in Am than *vice versa*, which is in good accord with the measured enthalpies of transitions for the mixture. There are two horizontals almost merging into one at about 1310 K. The shape of the predicted phase diagram closely resembles that of the Pu–Nd system studied by Ellinger *et al.* [19]. In their DTA measurements Ellinger *et al.* did not locate the liquid miscibility gap, which the editors of recent compilations have added with discretion [20]. The added miscibility gap, however, might be a little exaggerated.

Haire and Gibson [13] have also noticed depressions of Np transition temperatures by about 20 K, which the model calculation failed to predict. The invariant reaction involving the b.c.c.-Np and Np-rich liquid should be eutectic rather than peritectic. With a similar solubility of Nd in b.c.c.-Pu as that predicted for Am in b.c.c.-Np, the b.c.c.-Pu forms from the Pu–Nd liquid by a eutectic reaction.

Although the calculation could not reproduce the finer details of the experimental observation by Haire and Gibson, the general agreement as described above gives confidence in the Brewer model. Particularly with Am, it is important that the atomization energy to the gaseous valence state is used as the true measure of cohesive energy. Because of the special stability of the f^7s^2 ground state of Am, the atomization energy to the ground state gives too small a value as the measure of cohesive energy. Indeed, with the use of the atomization energy to the ground state as the cohesive energy, an extremely large liquid miscibility gap, whose critical temperature is about 2850 K, should be predicted for the Np–Am system [21].

3.3. Pu–Am

This system has been studied by Ellinger *et al.* [22] metallographically. They confirmed complete solid solubility between f.c.c.-Pu and f.c.c.-Am. Then, the existence of γ-Am was not known. They found that the solubility of Am in b.c.c.-Pu is limited to 8 at.% at 938 ± 15 K and located a peritectic reaction L+ f.c.c. $\rightarrow$ b.c.c.-Pu at that temperature.

Figure 5 shows the calculated high temperature phase diagram, which gives complete solid solubility not only between f.c.c.-Pu and f.c.c.-Am but also between b.c.c.-Pu and b.c.c.-Am. The interaction parameters for the liquid, b.c.c. and f.c.c. phases of this system are only

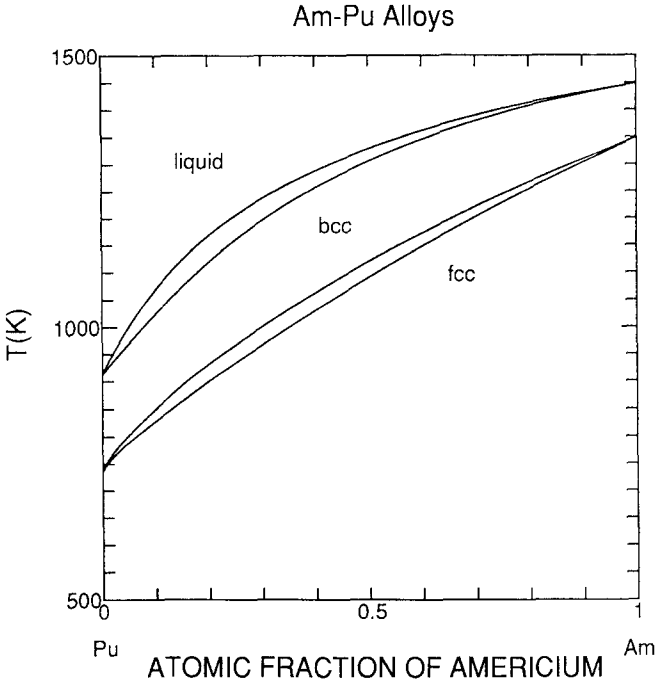

Fig. 5. Predicted phase diagram of the Pu–Am system.

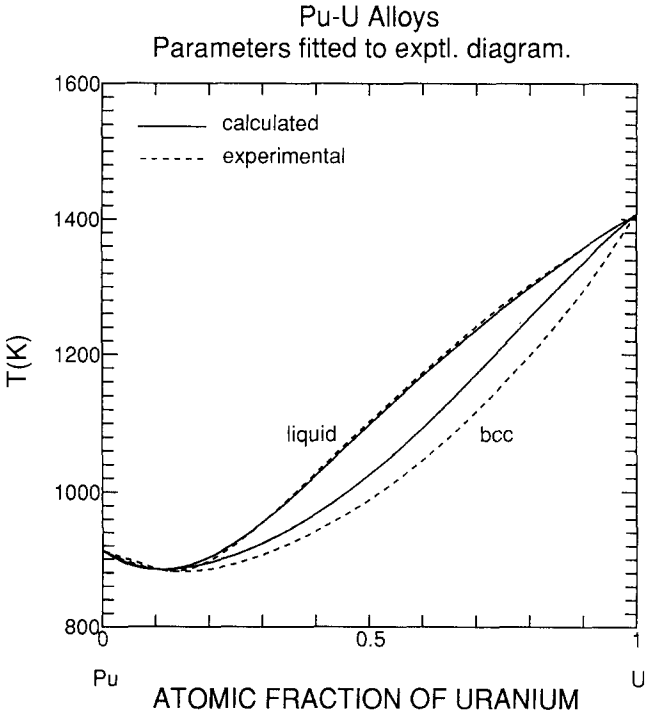

Fig. 6. Liquid–b.c.c. equilibrium in the U–Pu system.

about 1 kJ mol^{-1}. Either one of the following possibilities could explain the discrepancy between the calculated and experimental mutual solubilities of the b.c.c. metals.

(1) The structure of γ-Am is not b.c.c.

(2) There is a high temperature intermediate phase.

Both possibilities are considered not very likely. Now, the presence of γ-Am having been confirmed, further study at the Am-rich end is required. Also, studies on Am–Ln (Ln, lanthanides) systems such as Am–Nd would give valuable information on the structure and alloying behaviour of γ-Am.

3.4. U–Pu

From the practical point of view, this system is most important. Review and detailed thermochemical modelling have been done by Leibowitz *et al.* [23]. For this system, application of eqns. (2)–(5) failed to give the interaction parameter of correct magnitude: the predicted value was too positive by about 10 kJ mol^{-1}. Table 2 gives the interaction parameter for the b.c.c. phase of U–Pu alloys, which was derived from the experimental liquidus under the assumption that the liquid alloys are ideal solutions. The calculated and experimental solidus–liquidus curves are shown in Fig. 6 as solid and dashed curves respectively. The derived interaction parameter is a little different from that of Leibowitz *et al.* The ideality of the liquid alloys, which is assumed also by Leibowitz *et al.*, is somewhat arbitrary. A negative deviation from ideality as discussed by Chiotti *et al.* [24] considering the partitioning of Pu between Mg and U liquids is still possible.

In this study the Brewer valence bond model is applied in its most rudimentary form. There are several correction terms either explicit or implicit in his modelling of the Mo alloys [6]. Correction terms which give substantial negative contributions to the interaction parameters are related to (1) the charge transfer between the elements and (2) the better packing of different elements in a favourable size ratio. For instance, electrons on the crowded d-orbital of an element (*e.g.* Mo) could make use of the less crowded d-orbital of the other element (*e.g.* Zr). In practice, however, it is not straightforward to estimate these negative contributions to the interaction parameter. In order to understand the negative contributions to the interaction between the lighter actinides, the thermodynamic properties of the U–Pu system have to be studied.

3.5. U–Pu–Am and Np–Pu–Am

Several uncertain points have been identified in the modelling of the above binary systems. Nevertheless, the model is considered to give initial guidance on the alloying behaviour of the U–Pu–Am and Np–Pu–Am ternary systems. Since the interactions in the U–Pu and Pu–Am binaries are small, if any, the ternary alloying behaviour of the U–Pu–Am system would be largely determined by the interaction between U and Am. Similarly, the interactions in the Np–Pu and Pu–Am binaries are small compared with that between Np and Am. The interaction between Np and Pu is not trivial, but the excellent agreement of the calculated and experimental solidus–liquidus curves gives confidence.

Figure 7 shows the calculated liquidus surface of U–Pu–Am and Fig. 8 a calculated isotherm at 1200 K. Both the liquid and b.c.c. miscibility gap close rather rapidly with increasing Pu content. However, at about 10 at.% Pu, which is a probable Pu concentration in the fuel, the Am solubility in the U-rich alloys will be less than 10 at.% at 1200 K and will fall to less than 5 at.% below 1050 K. Since the tie-lines run parallel to the Am–U side, the Pu will be almost equally partitioned between the U-rich and Am-rich phases.

Figures 9 and 10 show calculated isotherms of Np–Pu–Am at 1000 and 1300 K respectively. Below 1000 K, Pu addition has little effect on the solubility

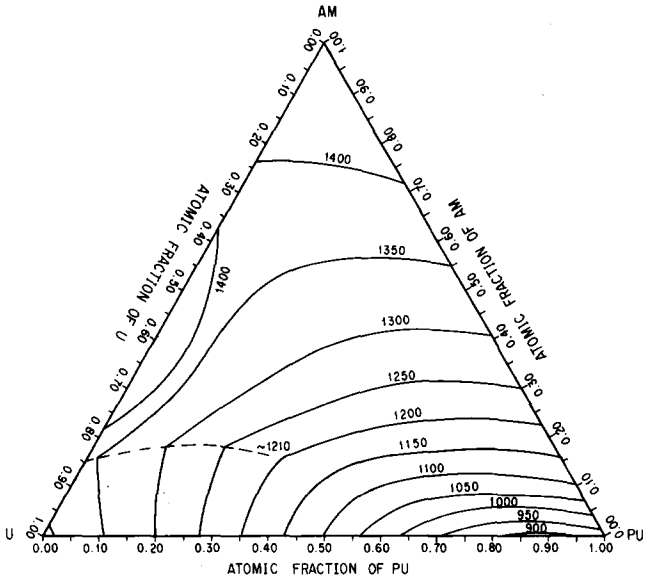

Fig. 7. Predicted liquidus projection of the U–Pu–Am system. Along the dashed curve the liquid alloy decomposes to the U-rich and Am-rich b.c.c. phases.

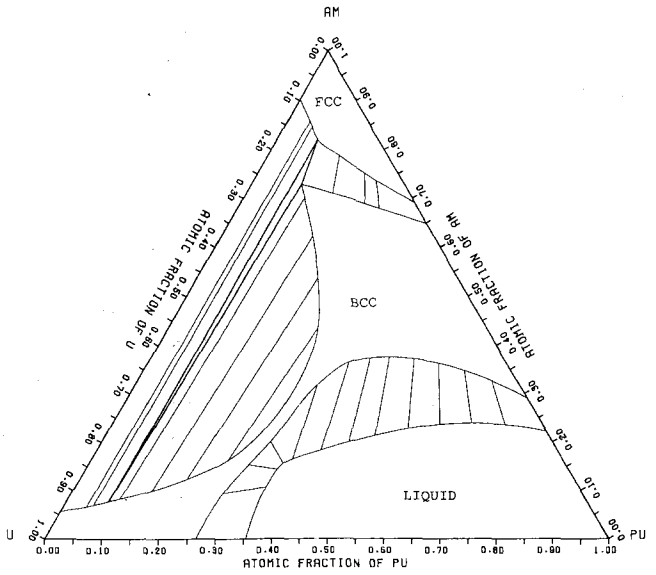

Fig. 8. Predicted isotherm of the U–Pu–Am system at 1200 K.

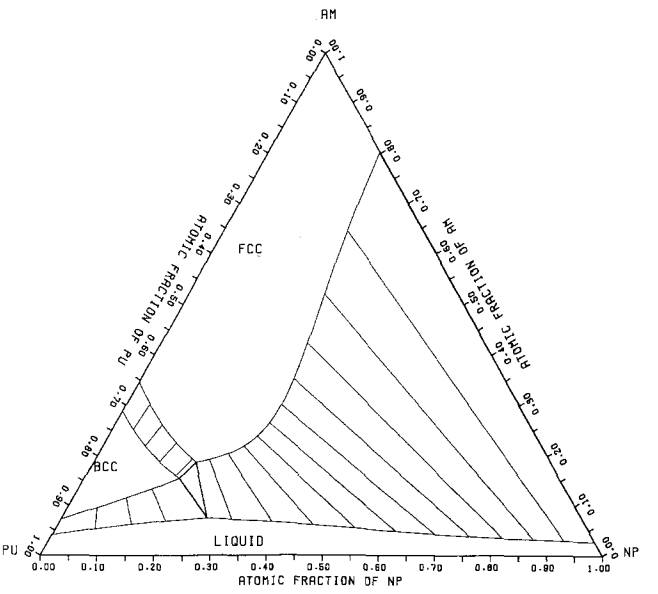

Fig. 9. Predicted isotherm of the Np–Pu–Am system at 1000 K.

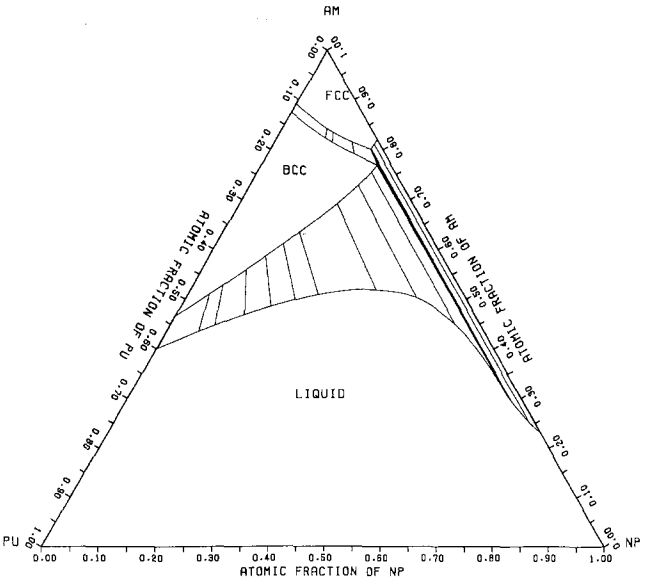

Fig. 10. Predicted isotherm of the Np–Pu–Am system at 1300 K.

of Am in Np-rich alloys. As in the Np–Am binary system, on heating above the melting point of Np, a predominantly Np melt will be formed with a solid residue consisting of an Am-rich phase.

4. Conclusions

The Brewer valence bond model was applied to predict the alloying behaviour among U, Np, Pu and Am. The calculated equilibria in the U–Np and Np–Pu binary systems agreed with the experimental phase diagrams. The predictions for the U–Am and Np–Am systems compared favourably with the recent experi-

mental observations on these systems. The model predicted the complete series of f.c.c. solid solutions in the Pu–Am system, which agreed with the metallographic observation on the alloys. However, there was a discrepancy between the calculated and experimental results on the solubility of Am in b.c.c.-Pu. The existence of γ-Am having been confirmed recently, this system warrants further study. Negative correction terms in the atomic interactions could be neglected for the above binaries but not for the U–Pu system. The nature and magnitude of the interaction between U and Pu have to be clarified. Since the interactions in the U–Pu, Pu–Am and Np–Pu binary systems were found to be small compared with those in the U–Am and Np–Am systems, the ternary alloying behaviour in the U–Pu–Am and Np–Pu–Am systems could be predicted.

Acknowledgments

I wish to thank Drs. R. G. Haire and J. K. Gibson, ORNL, for showing their data before publication, and Drs. M. Akabori and Y. Arai, JAERI, for discussing the materials. This study was made in conjunction with the Japan/US Actinide Program coordinated by Dr. T. Mukaiyama, JAERI, and Dr. S. Raman, ORNL. I would also like to thank Dr. L. Leibowitz, Argonne National Laboratory, for his comments.

References

1 D. R. Olander, S. Prussin, C. E. Johnson, J. N. Kass, Hj. Matzke, T. Ogawa, P. E. Potter, D. Powers and R. L. Yang, Reactor fuel technology, in E. K. Hulet (ed.), *Report of a Workshop on Transactinium Science, UCRL-LR-104538*, University of California, 1990, pp. 87–96.
2 L. Kaufman and H. Bernstein, *Computer Calculation of Phase Diagrams*, Academic, New York, 1970.
3 A. R. Miedema, F. R. de Boer and R. Boom, *Calphad, 1* (1977) 341.
4 L. Brewer, Viewpoints of stability of metallic structure, in P. Rudman, J. Stringer and R. I. Jaffee (eds.), *Phase Stability in Metals and Alloys*, McGraw-Hill, New York, 1967, pp. 39–61.
5 L. Brewer, in W. N. Miner (ed.), Thermodynamics and alloy behavior of the BCC and FCC phases of plutonium and thorium, *Plutonium 1970 and Other Actinides*, AIME, NY, 1970, p. 650.
6 L. Brewer and R. H. Lamoreaux, *At. Energy Rev., Spec. Issue No. 7* (1980) 11–194.
7 L. Brewer, *LBL-3720*, 1975 (Lawrence Berkeley Laboratory).
8 L. Brewer, *J. Less-Common Met., 133* (1987) 15.
9 Y. I. Chang and C. E. Till, Actinide recycle potential in the integral fast reactor (IFR) fuel cycle, in *LMR: A Decade of LMR Progress and Promise*, American Nuclear Society, La Grange Park, IL, 1991, pp. 129–137.
10 T. Mulaiyama, H. Takano, T. Takizuka, T. Ogawa, H. Yoshida and Y. Gunji, *ANS Trans., 64* (1991) 548.
11 R. H. Lamoreaux, *LBL-4995*, 1976 (Lawrence Berkeley Laboratory).
12 M. Hillert, *Calphad, 4* (1980) 1.
13 R. G. Haire and J. K. Gibson, *J. Nucl. Mater., 195* (1992) 156.
14 W. H. Zachariasen, *J. Inorg. Nucl. Chem., 35* (1973) 3487.
15 G. Eriksson and K. Hack, *Metall. Trans. B, 21* (1990) 1013.
16 P. G. Mardon and J. H. Pearce, *J. Less-Common Met., 1* (1959) 467.
17 P. G. Mardon, J. H. Pearce and J. A. C. Marples, *J. Less-Common Met., 3* (1961) 281.
18 T. Inoue, T. Matsumura, A. Sasahara, L. Koch and J. C. Spirlet, Transmutation of transuranium elements by a metallic fuel FBR, in *Proc. Information Exchange Meeting on Actinide and Fission Product Separation and Transmutation*, OECD Nuclear Energy Agency, Paris, 1990, pp. 397–423.
19 F. H. Ellinger, C. C. Land and K. A. Johnson, *J. Nucl. Mater., 29* (1969) 178.
20 T. B. Massalski, H. Okamoto, R. R. Subramanian and L. Kocprzak (eds.), *Binary Alloy Phase Diagrams*, Vol. 3, ASM International, Materials Park, OH, 1990, pp. 2799–2800.
21 E. C. Beahm, Oak Ridge National Laboratory, personal communication, 1989.
22 F. H. Ellinger, K. A. Johnson and V. O. Struebing, *J. Nucl. Mater., 20* (1966) 83.
23 L. Leibowitz, R. A. Blomquist and A. D. Pelton, *J. Nucl. Mater., 184* (1991) 59.
24 P. Chiotti, V. V. Akhachinskij, I. Ansara and M. H. Rand, *The Actinide Binary Alloys*, IAEA, Vienna, 1981, pp. 254–257.

Appendix

The Brewer model [6] gives the excess free energy of binary (i–j) alloys by

$$\Delta G^{E} = X_i X_j[(b+c) - (c/2)X_i] \quad \text{(A1)}$$

$$(b+c) = \alpha \quad \text{(A2)}$$

$$c = 2\alpha(V_i - V_j)/V_i \quad \text{(A3)}$$

where α is given in eqn. (2) in the text. Equation (A1) is compared with the RKM binary expression

$$\Delta G^{E} = X_i X_j[A_0 + A_1(X_i - X_j)]$$
$$= X_i X_j[(A_0 - A_1) + 2A_1 X_i] \quad \text{(A4)}$$

Hence,

$$A_0 = \alpha + A_1 \quad \text{(A5)}$$

$$A_1 = -(c/4) \quad \text{(A6)}$$

which are identical to those given by eqns. (4) and (5) in the text. The parameter β in eqn. (3), which is a function of molar volumes only, is employed.